Strike-slip kinematics in Central and Eastern Iran: Estimating fault slip-rates averaged over the Holocene

Bertrand Meyer[1] and Kristell Le Dortz[1]

Received 8 November 2006; revised 31 May 2007; accepted 14 June 2007; published 3 October 2007.

[1] According to GPS measurements, the right-lateral shear between Central Iran and Afghan blocks amounts to 16 mm/yr. A model based on very long-term estimates of fault-rates suggests the current shear originated about 5 Ma ago and has been accommodated by strike-slip faulting limited to the western (~2 mm/yr, Gowk-Nayband fault) and eastern (~14 mm/yr, Sistan system fault) edges of the Lut block. We have used high-resolution SPOT5 (pixel size 2.5 m) images to measure recent cumulative offsets and estimate slip-rates over shorter time periods that average several seismic cycles only. Recent offsets, a few tens of meters, have been found along the Anar fault inside the Central Iran plateau and along the Sistan faults east of the Lut. The offset-morphologies postdate the last incision of the network and are most probably of Holocene age (12 ± 2 ka). The corresponding slip-rates range between ~0.5–0.75 mm/yr, ~1.75–2.5 mm/yr, ~1–5 mm/yr, ~1–2.5 mm/yr for the Anar, East Neh, West Neh, and Asagie fault, respectively. These estimates suggest the GPS shear-rate across the Lut may not extrapolate over the Holocene. They also indicate strike-slip faulting is not confined to the Lut edges, but also occurs in Central Iran, suggesting the ongoing strike-slip tectonics might have originated between 8 and 22 Ma ago, earlier than considered previously and consistent with observations in NE Iran. **Citation:** Meyer, B., and K. Le Dortz (2007), Strike-slip kinematics in Central and Eastern Iran: Estimating fault slip-rates averaged over the Holocene, *Tectonics*, *26*, TC5009, doi:10.1029/2006TC002073.

1. Introduction

[2] The nature of deformation within active convergence zones has long been debated because of significant implications for the mechanical behavior and overall rheology of the continental lithosphere [e.g., *England and McKenzie*, 1982; *Tapponnier et al.*, 1982; *Jackson*, 2002; *Burov and Watts*, 2006]. Key aspects have concerned the relative amounts of distributed or localized deformations and the determination of fault kinematics. Attention has been focused on the large strike-slip faults of Tibet and Central Asia [*Molnar and Tapponnier*, 1975; *Tapponnier and Molnar*, 1977] with emphasis on determining slip-rates, amount of geologic offset and inception of faulting [e.g., *Armijo et al.*, 1989; *Peltzer et al.*, 1989; *Avouac and Tapponnier*, 1993; *England and Molnar*, 1997; *Leloup et al.*, 1995; *Meyer et al.*, 1998]. Theoretically, a variety of displaced markers with ages uniformly distributed throughout time provide independent determinations of total offset, fault inception, and slip-rates (Figure 1). A similar offset recorded by markers of different ages would provide the total offset, and the oldest of the cumulative offsets with a smaller displacement, the onset of faulting. Decreasing offsets with younging ages would provide the evolution of slip-rate since inception of motion and over different periods. Generally, critical observations (i.e., well determined offsets of a given age) are relatively few, leaving uncertainties. An estimate of the total offset is usually combined with short-term (Holocene, 12 ± 2 ka) or longer-term (Pleistocene, ≤1.81 Ma) geologic rates to infer the inception of deformation. Short-term geodetic slip-rates either derived from GPS measurements or from Insar techniques can be used in a similar way to infer the onset of deformation. When short-term geologic and geodetic slip-rates are comparable, they provide close estimates of the inception of deformation and are equally appropriate although both span a much shorter period than that involved in the duration of deformation and remain short of evidencing variations over the long-term (Figure 1). Short-term geologic and geodetic slip-rates may nonetheless differ with possible consequences for the assessment of fault inception. For example, there is an enduring discrepancy for the Altyn Tagh Fault between millennial geologic slip-rates of ~20–30 mm/yr [e.g., *Peltzer et al.*, 1989; *Mériaux et al.*, 2004, 2005] and decadal geodetic slip-rates of ~5–9 mm/yr with Insar [*Wright et al.*, 2004] or GPS [*Bendick et al.*, 2000; *Wallace et al.*, 2004] techniques. When short-term geologic and geodetic slip-rates are different and whatever the reasons for it [e.g., *Friedrich et al.*, 2003], the use of the rate that integrates several seismic cycles and averages the longer time period appears more appropriate to estimate inception of faulting.

[3] We address these questions for major strike-slip faults in Central and Eastern Iran where geodetic information is available but Holocene kinematics lacking. The area of interest is located within the Arabia-Eurasia convergence zone, between 53–61°E (Figure 2). At 58°E, a transition occurs between widespread collision to the west, and a narrow subduction zone to the east (Figure 2). The differential motion between the already colliding and yet subducting domains is well determined from GPS studies [*Vernant et al.*, 2004] and amounts to 16 mm/yr of N-S

[1]Laboratoire de Tectonique, Université Pierre et Marie Curie, Paris, France.

0278-7407/07/2006TC002073$12.00

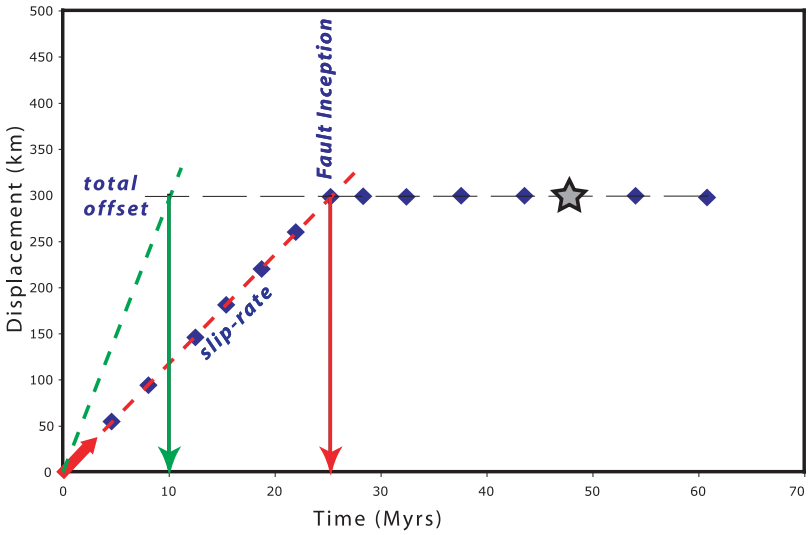

Figure 1. Fault displacement versus time. Ideal case where a variety of offsets with distributed ages (blue diamonds) allows an independent determination of slip-rate, total offset, and inception of faulting. In usual cases, a short-term slip-rate is extrapolated back through geological time and combined with a single estimate of the finite offset (star) to infer faulting inception. Most often, Holocene and GPS slip-rates are found comparable (oblique red arrow not to scale) and provide a similar faulting inception (dashed red-line and corresponding vertical arrow). Accounting for the possibility that the geodetic and geologic slip-rates differ, extrapolating the GPS slip-rate may provide an inadequate estimate of faulting inception (green dashed-line and corresponding vertical arrow). See text for discussion.

right-lateral shear at 30.5°N (difference between the vectors KERM and ZABO, inset Figure 2, Figure 3). This differential motion is thought to be accounted for by prominent dextral faults bounding the Lut, but the loose GPS network cannot determine the interseismic strain accumulation across given faults nor elucidate the relative contributions of the eastern and western edges of the Lut. Holocene and/or Pleistocene fault slip-rates remain mostly unknown and the description of the Late Tertiary regional kinematics relies on the 5–7 Ma-old onset of deformation assumed by *Walker and Jackson* [2004]. Our primary objectives are to estimate Holocene slip-rates and hence investigate the kinematics over a period averaging several seismic cycles. We summarize the regional geology and discuss the basic assumptions of the kinematic model of *Walker and Jackson* [2004]. We then use high-resolution SPOT5 imagery (pixel size 2.5 m) to provide evidence for right-lateral offsets of recent alluvial fan systems along the Anar and Eastern Lut faults. We discuss the plausible ages of these recent offsets by investigating a regional morphoclimatic scenario compatible with the evolution of similar fan systems dated 300 km to the south as well as 500 km to the north. We finally provide rough estimates of Holocene slip-rates and discuss our observations in the framework of the Tertiary tectonic evolution of southern Iran.

2. Tectonic Setting and Previous Kinematics Model

[4] Iran has a long and rather complex tectonic evolution related to the multistage history of the Tethys domain. The accretion of small continental blocks of Gondwanian affinity to Eurasia (Lut, Afghan, and Central Iran sometimes subdivided into Yadz and Tabas blocks) has resulted from successive opening and closure of large oceanic domains or narrow back-arc and marginal basins. The closure of the Paleo-Tethys is denoted by sparse ophiolitic remnants associated with Early Jurassic accretion to Eurasia [e.g., *Berberian and Berberian*, 1981; *Berberian and King*, 1981]. The Late-Cretaceous Early Tertiary closure of several Neo-Tethys oceanic domains is attested to by the emplacement of younger and more continuous sutures: Nain Baft (NB) between Central Iran and Sanandaj Sirjan to the south, Sabzevar (SB) between Central Iran and Eurasia to the north, and Sistan between Lut and Afghanistan to the east (inset of Figure 2). Emplacement of the Urumieh-Dokhtar magmatic arc occurred later during Eocene-Oligo-

Figure 2. LANDSAT Mosaic of the major active strike-slip faults of Central and Eastern Iran. Boxes locate Figures 4 and 7. Red boxe indicates location of Figure 12 along the Sabzevaran faulted piedmont. Inset is a simplified sismotectonic map of Iran. Ophiolite outcrops and sutures are stylized (NB, Nain Baft; Sb, Sabzevar; S, Sistan) Overall Arabia-Eurasia convergence [*Sella et al.*, 2002] and GPS velocities relative to stable Eurasia [*Vernant et al.*, 2004] are indicated by grey and red arrows, respectively.

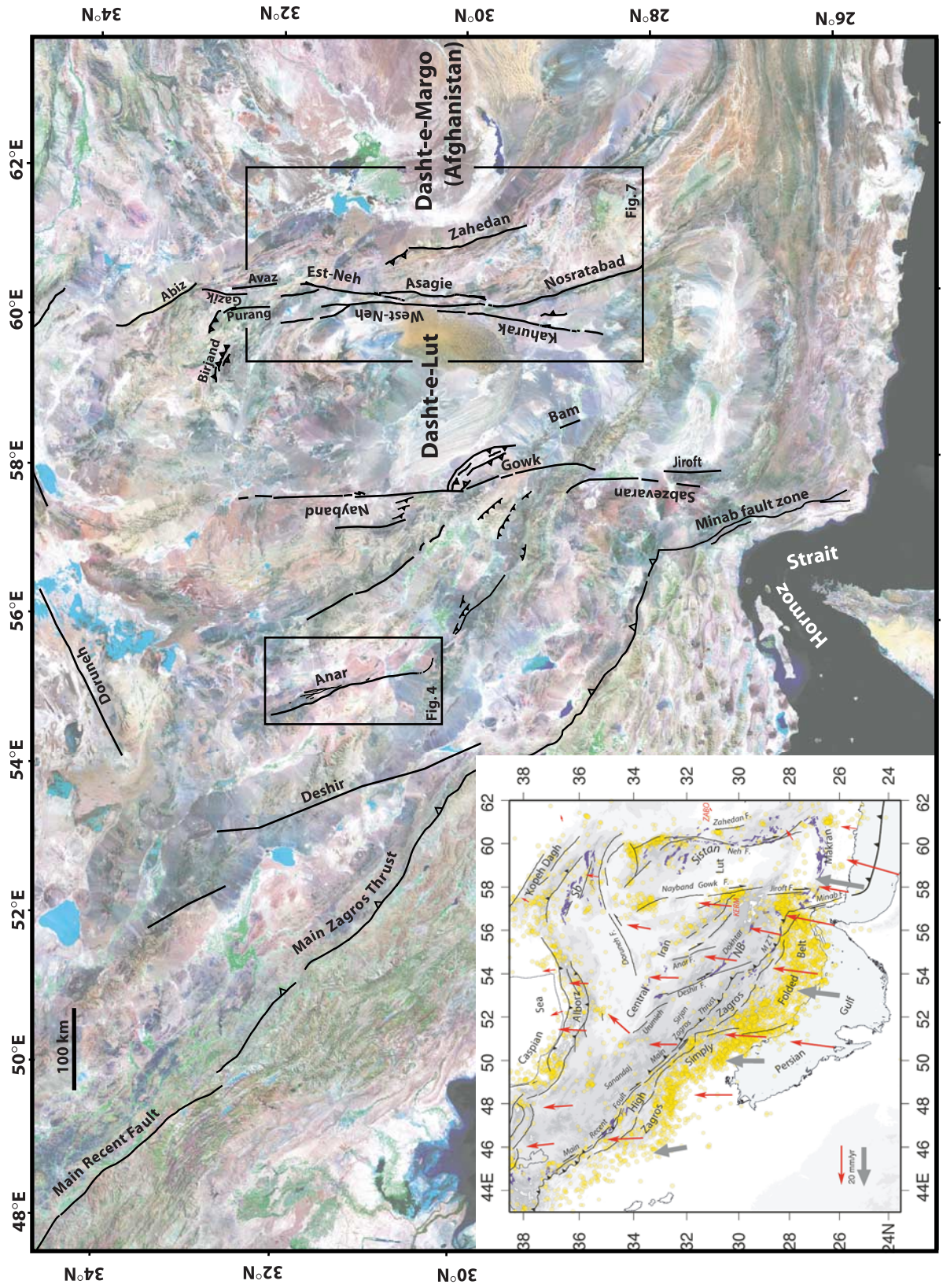
Dasht-e-Margo (Afghanistan)
Dasht-e-Lut
Fig.7
Zahedan
Abiz
Avaz
Est-Neh
Asagie
Nosratabad
Gazik
Purang
West-Neh
Kahurak
Birjand
Bam
Gowk
Jiroft
Sabzevaran
Nayband
Minab fault zone
Strait
Hormoz
Anar
Fig.4
Dornuneh
Deshir
Main Zagros Thrust
Main Recent Fault
100 km
62°E
60°E
58°E
56°E
54°E
52°E
50°E
48°E
34°N
32°N
30°N
28°N
26°N
Sistan
Lut
Kopeh Dagh
Makran
Caspian Sea
Alborz
Central Iran
Folded Belt
Simply Folded Zagros
Persian Gulf
High Zagros
20 mm/yr

Figure 2

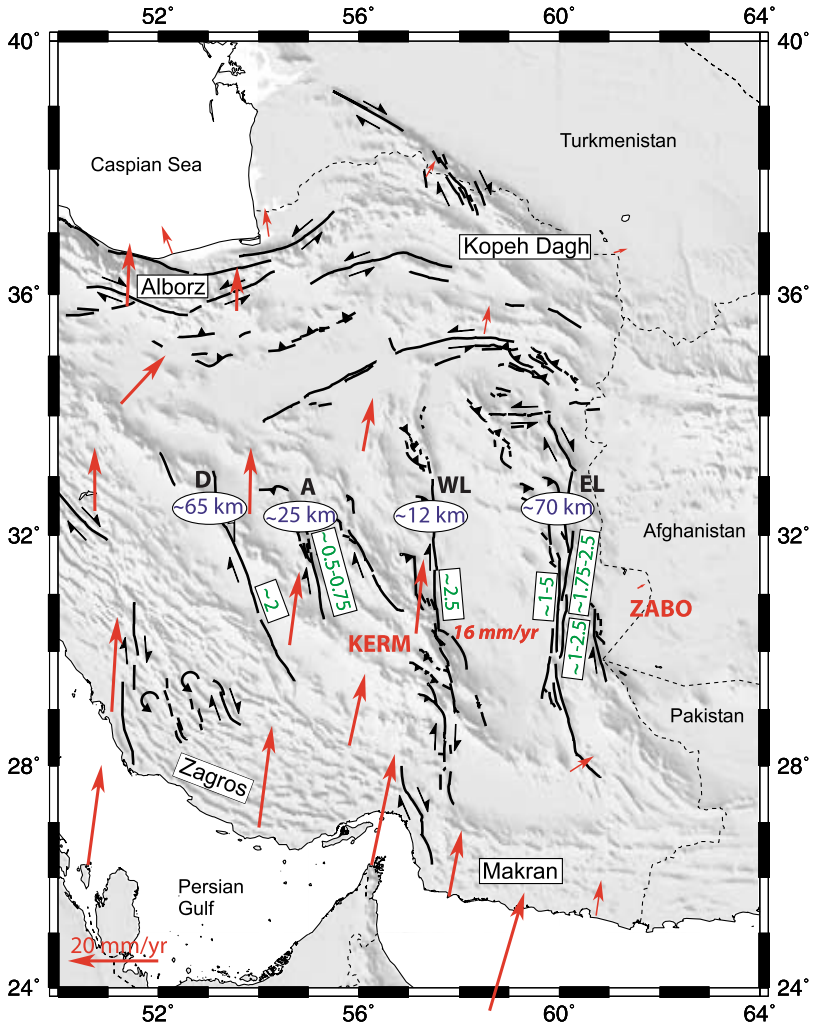

Figure 3. Strike-slip faulting in Central and Eastern Iran. Modified from *Walker and Jackson* [2004]. Total offsets across Deshir (D), Anar (A), West Lut (WL), and East Lut (EL) faults are indicated in km. GPS velocities relative to stable Eurasia [red arrows, *Vernant et al.*, 2004] indicate ~16 mm/yr of right-lateral shear across WL and EL fault systems. Slip-rate on individual faults (green numbers in mm/yr) is averaged over the Quaternary for West Lut [*Walker and Jackson*, 2002] and the Holocene for Deshir [*Meyer et al.*, 2006], Anar and East Lut (this study).

cene times and relates to the long lasting northward subduction of Neotethys under Central Iran [*Berberian et al.*, 1982; *Agard et al.*, 2006]. Calc-alcaline plutonic rocks and associated volcanites that overlie and/or intrude the Nain-Baft suture occurred before the emplacement of the Main Zagros Thrust (MZT) suture zone and the accretion of the Arabian margin to Eurasia. The Neo-Tethys subduction has evolved into a collisional stage NW of the Hormoz strait but remains active to the south, offshore Makran. The closure of MZT and the very onset of the collisionnal stage, are difficult to date but are thought to have occurred about 35 Ma ago [e.g., *Agard et al.*, 2005]. The collision of Iran with Arabia has given rise to the Iranian plateau and the Zagros mountains. The occurrence of Oligo-Miocene reefal limestones on the plateau (Qom formation) and within the Zagros (Asmari-Jahrom formations) indicates the entire region remained close to sea level until the middle of the Tertiary, ~20 Ma ago, and reached its current elevation since then. The processes involved in the construction of the topography are probably diachronous since deformation of the outer Zagros has taken place in the last 8 Ma [*Homke et al.*, 2004] with main folding taking place during the last 5 Ma [e.g., *Talebian and Jackson*, 2002, 2004]. The long NNW-SSE strike-slip faults within the Iranian plateau (Deshir, Anar) and along the edges of the Lut (Gowk-Nayband-Bam, Neh-Asagie-Kahurak-Zahedan) offset all but the MZT suture zone, and relate to the ongoing collisional stage. Hence the inception ages and slip-rates of these strike-slip faults are important for discussing the timing of construction of the relief and the evolution of regional kinematics.

[5] *Walker and Jackson* [2002, 2004] provided a detailed description and a thorough discussion of the total strike-slip offsets across the Gowk (~12–15 km) and the Sistan (~70–

Table 1. Slip–Rate Estimates for the Main Strike–Slip Faults of Central and Eastern Iran[a]

	Central Iran		West Lut	Sistan = East Lut		
Slip-Rate	Deshir	Anar	Gowk-Nayband	Wet-Neh and Kahurak	East Neh and Asagie	Zahedan
Short-term (4 years) GPS -derived slip-rate [*Vernant et al.*, 2004]	0	0		Σ = 16 mm/yr		
Geological offset (km)	65 ± 15 km	**25 ± 5 km**	~12–15 km	~10 km	~50 km East Lut: $\Sigma \sim$ 70 km	~13–20 km
Inferred fault inception	~20 Ma	**~20 Ma**	~5 Ma	~5 Ma	~5 Ma	~5 Ma
Very long-term slip-rate	~2.5–4 mm/yr [*Meyer et al.*, 2006]	**~1–1.5 mm/yr**	~2.4 mm/yr [*Walker and Jackson*, 2002]	[*Walker and Jackson*, 2004]	East Lut: $\Sigma \sim$ 14 mm/yr [*Walker and Jackson*, 2004]	[*Walker and Jackson*, 2004]
Long-term geologic Pleistocene slip-rate (~100 ka to ~2 Ma)			≥1.5 mm/yr [*Walker and Jackson*, 2002]			
Short-term geologic	~2 mm/yr	**~0.5–0.75 mm/yr**		West Neh ~1–5 mm/yr	East Neh ~1.75–2.5 mm/yr	
Holocene slip-rate (~12 ka)					Asagie ~1–2.5 mm/yr	

[a]Short-term geodetic slip-rates are obtained from two GPS campaigns, 4 years apart. Very long-term slip-rates combine the estimate of the total offset with the inferred time of fault inception. Long-term (Pleistocene) and short-term (Holocene) geologic slip-rates combine quaternary offsets of known or inferred age. Boldface figures are related to this study.

95 km) fault zones. Following the assumption by *Allen et al.* [2004] that the current stage of deformation initiated 5 ± 2 Ma ago, *Walker and Jackson* [2004] integrated the comparison between the long-term geologic offsets and short-term geodetic motions into a Late Tertiary kinematic model. The model assumes that during the last 5–7 Ma, right-lateral shear between Central and Eastern Iran had remained confined by the edges of the Lut with little motion to the west, within the Iranian plateau. Figure 3 summarizes the findings of *Walker and Jackson* [2004]. Summing the most likely values of the total offsets across the Sistan suture zone (Neh and Zahedan faults, ~70 km) and the Gowk-Nayband system (~12–15 km), they deduced a long-term shear-rate of 12–17 mm/yr similar to the ~16 mm/yr deduced from the GPS. Accounting for the modest internal deformation the GPS allows within Central Iran, they inferred limited activity along the Anar and Deshir faults and postulated that their total offsets had mainly accrued before ca 5 Ma. Their model therefore postulates that the current shear between Central and Eastern Iran results from ~2 mm/yr (Gowk-Nayband faults) and ~14 mm/yr (Sistan faults) of right-lateral slip along the edges of the Lut block. With the exception of the Nayband fault, for which a 3.2 km-offset of a river entrenched in a 2.1 Ma-old basaltic flow provides a minimum Pleistocene slip-rate of 1.5 mm/yr [*Walker and Jackson*, 2002], fault-rates discussed by *Walker and Jackson* [2004] are either short-term GPS-derived or very long-term geologic estimates (Table 1). These rates are dependent on the basic assumptions made; both the inception of deformation at 5–7 Myrs ago, and the reliability of GPS velocities extrapolated over geologic timescales may be questioned.

[6] Recent geomorphic studies within the Central Iran plateau [*Meyer et al.*, 2006] demonstrated the ongoing activity of the Deshir fault, 250 km west of the Gowk-Nayband system. The smallest cumulative offsets documented suggest the Deshir fault slips at a Holocene rate of ~2 mm/yr and has accumulated its total offset of 65 ± 15 km over a period longer than the last 5 Ma. This indicates that right-lateral shear between Central and Eastern Iran may have affected a wider region and started earlier than anticipated by *Walker and Jackson* [2004]. These recent observations further indicate that the assessment of the regional kinematics cannot rely solely upon geodetic or very long-term geologic slip-rates and deserves the determination of fault slip-rates integrating several seismic cycles. The Holocene slip-rate estimates from this study have been reported in Figure 3 and Table 1 to avoid duplication of figures and to allow an easy comparison with the GPS displacement field. The following two sections document the Late Quaternary offsets along the Anar fault, within the Iranian plateau, and along the Sistan fault zone, east of the Lut.

3. Strike-Slip Faulting Within the Iranian Plateau: The Anar Fault

[7] The Anar fault is a 200 km-long right-lateral strike-slip fault that is parallel to the Deshir fault to the east (Figure 2). The fault is located within the Central Iran

plateau and lies 250 km west of its eastern edge marked by the Nayband-Gowk fault system. The northern portion of the fault is made of several NNW-SSE closely spaced splays cutting across the structure and the morphology of Kuh-e-Kharanaq mountains (Figure 4). The splays merge southwards into a single and localized fault strand that cuts obliquely across Kuh-e-Bafq mountains and southwestern piedmont. The southern portion crosses the Anar salt flat and vanishes north of the Urumieh Dokhtar magmatics, where the fault bends eastward to reactivate a north-dipping thrust in the Kuh-e-Mosahem mountains. Geologic offsets have been documented across the northern and southern fault portions [e.g., *Nabavi*, 1970; *Walker and Jackson*, 2004] both cutting across structural units and displacing a series of NW-SE trending folds. The offset folds involve Jurassic-to-Middle Palaeogene sedimentary units and indicate inception of strike-slip motion later in the Tertiary. The northern fault portion offsets steeply dipping conglomeratic units and the right-lateral motion summed across the distinctive splays amounts $\sim$10 km (Figure 4). Offset of a distinct sandstone unit intercalated within Lower Cretaceous shales indicates a 25 $\pm$ 5 km right-lateral offset on the southern fault portion, and provides a likely estimate of total displacement accumulated across the Anar fault [e.g., *Walker and Jackson*, 2004].

[8] Morphological evidence of recent motion is found along the southern strand where the fault cuts across the Quaternary piedmont of Kuh-e-Bafq and the Anar salt flat (Figure 4). The east-facing scarp denoted by *Walker and Jackson* [2004] within ancient alluvium of the salt-flat (see their Figure 11c) is almost 30 m high based on SRTM topographic data. This step denotes a minor vertical component of slip and might be coeval with the larger, 900 m dextral deflection of the northern limit of the salt-flat (Figure 4). The evidence for the most recent faulting activity is found north of Anar where the fault disrupts a series of coalescent fans merging downstream with the salt flat depression (Figure 5). The relative ages of the fans can be estimated from their relative elevation and degree of incision by the active streambeds. The surface of the piedmont mainly corresponds to the most recent fan system. The drainage network outlines the active depositional lobes of the fans whose braided channels and river floodplains have incised the inactive parts (yellow shading, Figure 5) by a few meters at most. Older surfaces preserved in a few places (orange shading) have been incised by numerous ephemeral streams and by tributaries of the active network. They either correspond to a preceding fan system or to older alluviums deposited while aggradation of the fan was taking place. Although the fault is scarcely discernible on LANDSAT imagery (28.5 m multispectral plus 14.25 m panchromatic bands), it is clearly seen on the SPOT5 imagery (2.5 m multispectral bands), owing to the higher resolution which reveals subtle morphological details. Except for the main river floodplains where it has been erased by erosion, a scarp, most often facing west, outlines the trace of the fault. The scarp is subdued, undetected on topographic profiles using SRTM data, and a few meters high at most. Two sites display clear evidence for recent right-lateral cumulative offsets. Site 1 locates at the contact between recent alluvium and abraded bedrock of Kuh-e-Bafq mountains. The fault cuts obliquely across a large river floodplain incised within the recent fan system (Figure 5b). East of the fault, the fan deposits mantle the basement rocks or surround elongated hills denoting the structural trends oblique to the fault. West of the fault, the fan deposits appear thicker and the structural trends are no longer discernible. Looking west, the right bank of the river, illuminated by the sun, is cleanly offset while the left bank, shaded, is not. This is common for right-lateral faults that often preserve right bank offsets and tend to erase left bank ones. The offset of the right bank amounts to 7.5 m and appears similar to that of two small gullies incised within the fan surface south of the left bank. The resolution of Quickbird imagery (60 cm panchromatic band) exemplifies the offset of the riser (Figure 6a), and confirms the reliability of the measurement obtained with the SPOT5 data. The photograph of Figure 6b highlights the sharpness of the offset-riser with the upstream and downstream banks of the river abutting against the fault scarp at right angle. Site 2 locates further to the south where the fault cuts across the middle of the piedmont (Figure 5c). Two abandoned alluvial surfaces can be distinguished. One appears similar to that of site 1 and has incised an older surface. Both surfaces are cut by the fault whose trace appears on the SPOT5 enlargement as a NE-SW narrow dark stripe. The scarp is oblique to the overall direction of the small intermittent streams flowing to the southwest. Across the older surface, there is no obvious continuity between the streams east of scarp and the streams west of it. The former seem to have been cut from their headwaters while the latter were offset and eventually drained south-eastward along scarp. Removing about 15–20 m of dextral fault motion aligns the upstream and downstream courses of most of the channels incised in the upper surface. A larger stream to the north that incises both the upper and lower surfaces is also displaced. The offset (right inset in Figure 5c) is difficult to estimate but appears smaller than the 15–20 m offset of the rills on the upper surface. The use of Quickbird data helps illustrating these offsets and allows measuring $\sim$8 m of right-lateral displacement for the smaller one (Figure 6c). The sharpness of the offset is clear in the field and the steepness of the riser indicates it corresponds to the last incision of the network (Figure 6d). The former observations indicate the Anar fault has accumulated about 15–20 m of dextral slip since the abandonment of the upper surface, almost twice that accumulated since the abandonment of the lower surface and the latest incision of the network.

4. Strike-Slip Faulting East of the Lut: The Sistan Faults

[9] The Sistan fault system outlines the N-S boundary between the Dasht-e-Lut and Dasht-e-Margo deserts (Figure 2). The system is about 400 km long and comprises several right-lateral strike-slip faults truncating the lowlands of Lut and Afghanistan and the intervening East Iranian ranges [*Berberian et al.*, 1999, Figure 7; 2000; *Walker and*

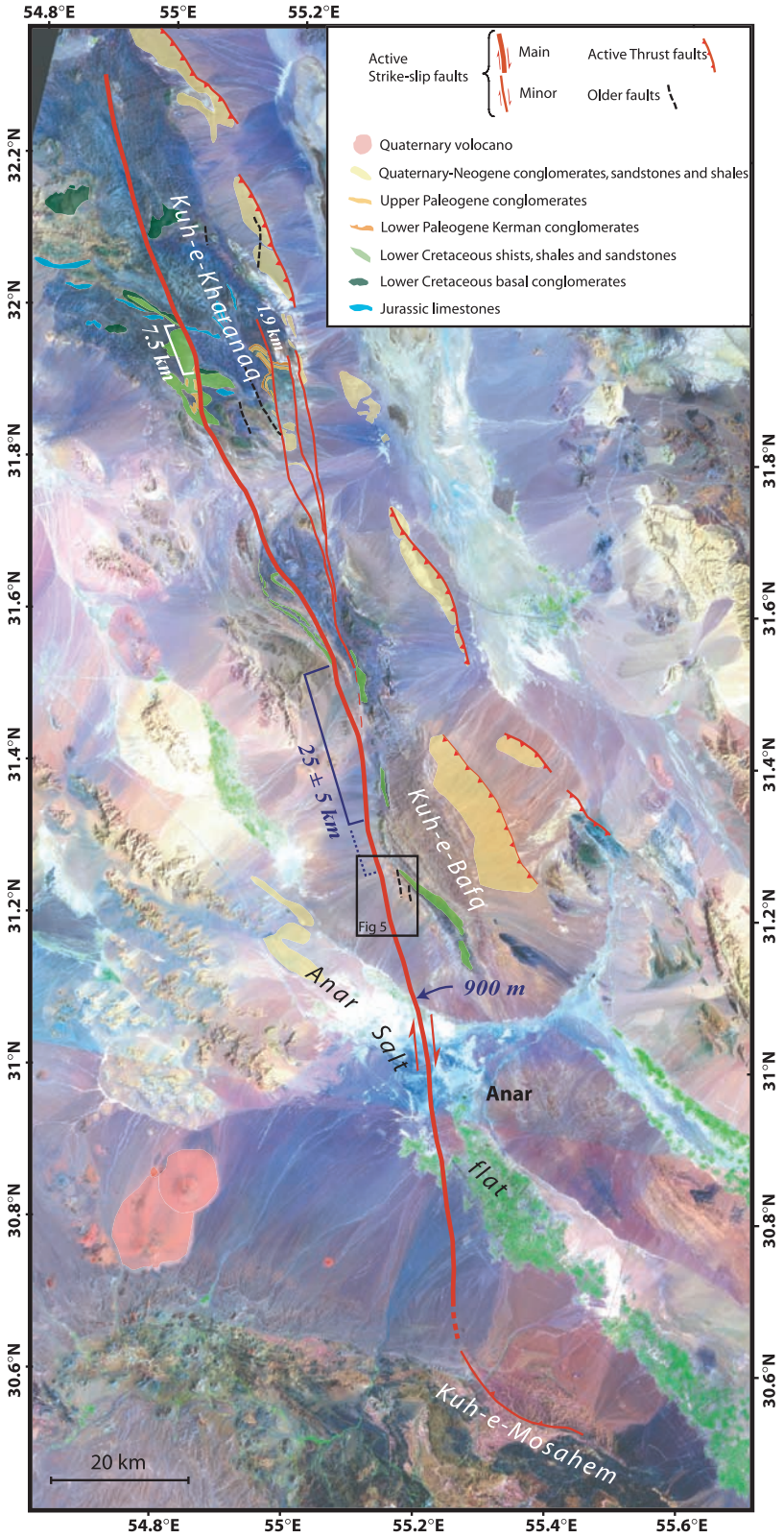

Figure 4. LANDSAT Mosaic of the Anar fault. Geologic information is reported from Yazd [*Nabavi*, 1970] and Ardekan [*Valeh and Haghipour*, 1970] 1/250.000 GSI maps. Offsets of distinctive units are denoted. White arrow near 31°N indicates a right-lateral deflection of salt-flat border. Box indicates location of Figure 5a.

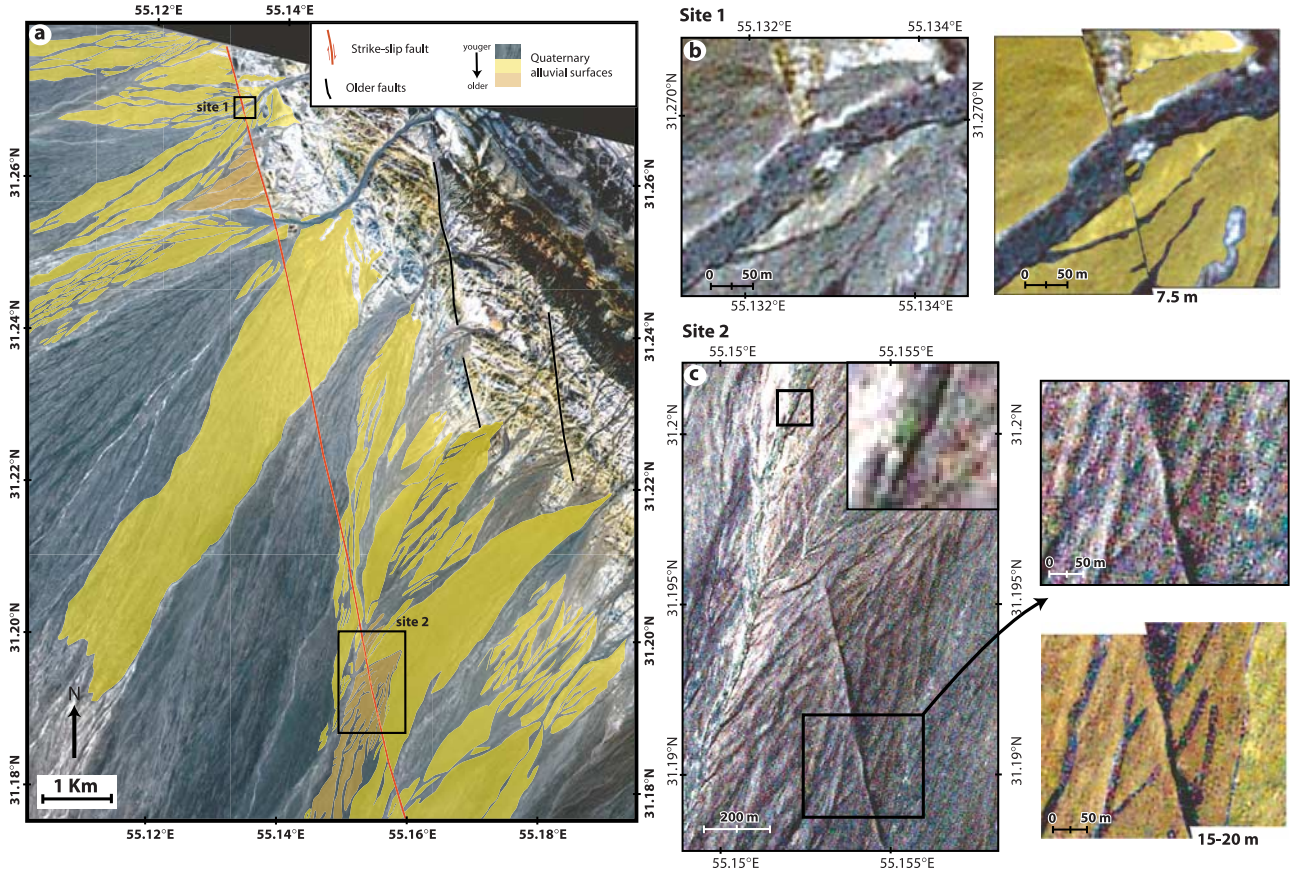

Figure 5. SPOT5 imagery along the southern portion of the Anar fault. (a) Fault trace cutting across the Quaternary piedmont. Channels and main river floodplains incise the youngest fan system (yellow shading) and the remains of an older one (orange shading). Boxes indicate location of site 1 (b) and site 2 (c), and location of Figures 6a and 6c Site enlargements point to recent cumulative offsets mostly coeval with the last incision of the network (left panels) with corresponding right-lateral motion restored (right panels).

Jackson, 2004]. The ranges involve two different accretionary prisms, the Neh and Ratuk complexes, often designated as the Sistan suture and thought to represent the remains of a former Neo-Tethys domain [e.g., *Tirrul et al.*, 1983]. The closure of that domain involved several phases of Late Cretaceous - Early Tertiary deformations and took place before the inception of the current strike-slip tectonic stage. The Sistan faults cut obliquely across the East Iranian ranges and offset several distinctive units of the suture. The geologic offsets on Figure 7 are reported from the detailed mapping of *Walker and Jackson* [2004], from which basic structural and stratigraphic information can be retrieved. These offsets provide likely estimates of the total offset since the inception of the strike-slip tectonics. The eastern side of the Lut that includes the East Neh, West Neh, Asagie, Kahurak, and Nosratabad faults has accumulated a larger offset (~60 km) than the Zahedan fault (~13–20 km) which lies 50 km east, bounding the Afghan lowlands. Consequently, we focused on the Eastern Lut and searched for offset morphologies where the faults disrupt recent alluvium on the available SPOT5 imagery. Between 30°N and 31.5°N, 14 sites (Figure 7 and Table 2) provide evidence for recent right lateral offset. Most of the sites concern the East Neh, West Neh, and Asagie faults and only one the Kahurak fault. The sites and corresponding offsets are described in Figures 8–11.

[10] Three sites locate along the East Neh fault (E1–E3 in Figure 7, and Table 2). Site E1 locates near 31.5°N along the northern portion of the East Neh fault where it cuts across the eastern piedmont of the Nasfandeh Kuh range (Figure 7). The fans that cover most of the piedmont have a dark-brown uniform hue on the SPOT5 image (Figure 8a). To the south, they are well preserved and have only been incised by intermittent streams denoted by a light-brown hue. To the north, the fans are more dissected and have been incised both by intermittent streams and by the river floodplains of the contemporary drainage. The fault disrupts the drainage and the offset accumulated since the incision of the fan surface amounts to 25 m. Site E2 locates ~25 km further to the south. There, the East Neh fault cuts across basement and disrupts the east-west trending drainage system. The fault runs in the middle of the SPOT5 extract (Figure 8b). The enlargement highlights the course of a large river whose main river floodplain shows ~25 m of

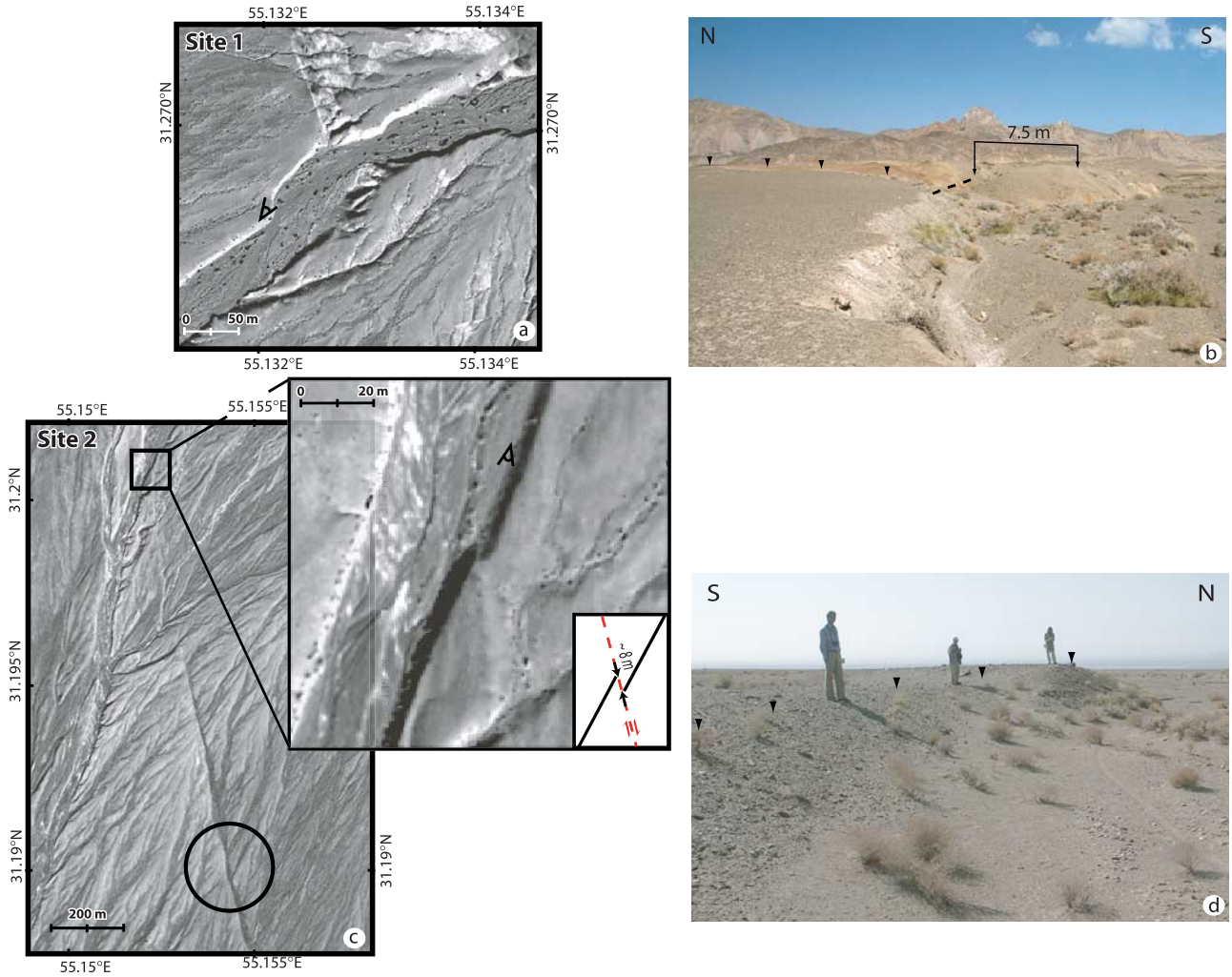

Figure 6. Quickbird imagery (a and c; see Figure 5 for location) and field photographs (b,d) of the Anar fault at site 1 (top) and site2 (bottom). The resolution (pixel size 0.6 m) exemplifies the offsets denoted with the SPOT5 data. The photographs outline the steepness of the offset-risers. Black triangles point to fault trace (c) or top of offset-riser (d). For site 2, circle and square with enlarging respectively denote the offset-rills and the offset-riser of Figure 5c.

dextral offset. Site E3 locate ~20 km further to the south where the fault runs across a series of alluvial fans (Figure 8c). The active fan system that locates east of the fault appears with a blue-grey hue on the color composition. Older fans crop out nearby the fault and have either light beige or dark brown hues. The enlargement shows a small stream that has incised the older fans to the base level of the active ones. The course of the stream indicates ~25 m of dextral-offset. This suggests the slip accumulated since the last regional incision of the drainage does not fluctuate much along strike for the East Neh fault.

[11] This is also the case for the Asagie fault, often considered as the southern portion of the East Neh fault. For the Asagie fault, three of the four sites that display recent cumulative displacements of the youngest fans are suggestive of a 25 m offset (A1–A3 in Figure 7, and Table 2). Site A1 locates about 35 km to the south of site E3, along the northern part of the Asagie fault, where it cuts across intermittent streams and intervening ridges (Figure 9a). The streams flow eastward from basement rocks (dark blue) to incise a Plio-Quaternary apron (light brown). The streams merge further east with the active drainage system outside the area covered in Figure 9a. The enlargement highlights a series of dextral offsets compatible with ~25 m of fault-motion since the incision and the coeval shaping of the ridges. Site A2 locate 6 km further to the south where the Asagie fault cuts across the upper reach of an east dipping piedmont mantling basement rocks (Figure 9b). The active fan system, denoted by light grey hues, covers most of the area to the south. Older fan systems cover most of the area to the north and appear with darker brown hues. Several meandering streams have incised the older fans to join the floodplains of the active network. The two largest streams are offset in a right-lateral sense. Restoring about 25 m of dextral fault-motion removes the bayonet-shaped portion of the southern stream and aligns the upstream and downstream

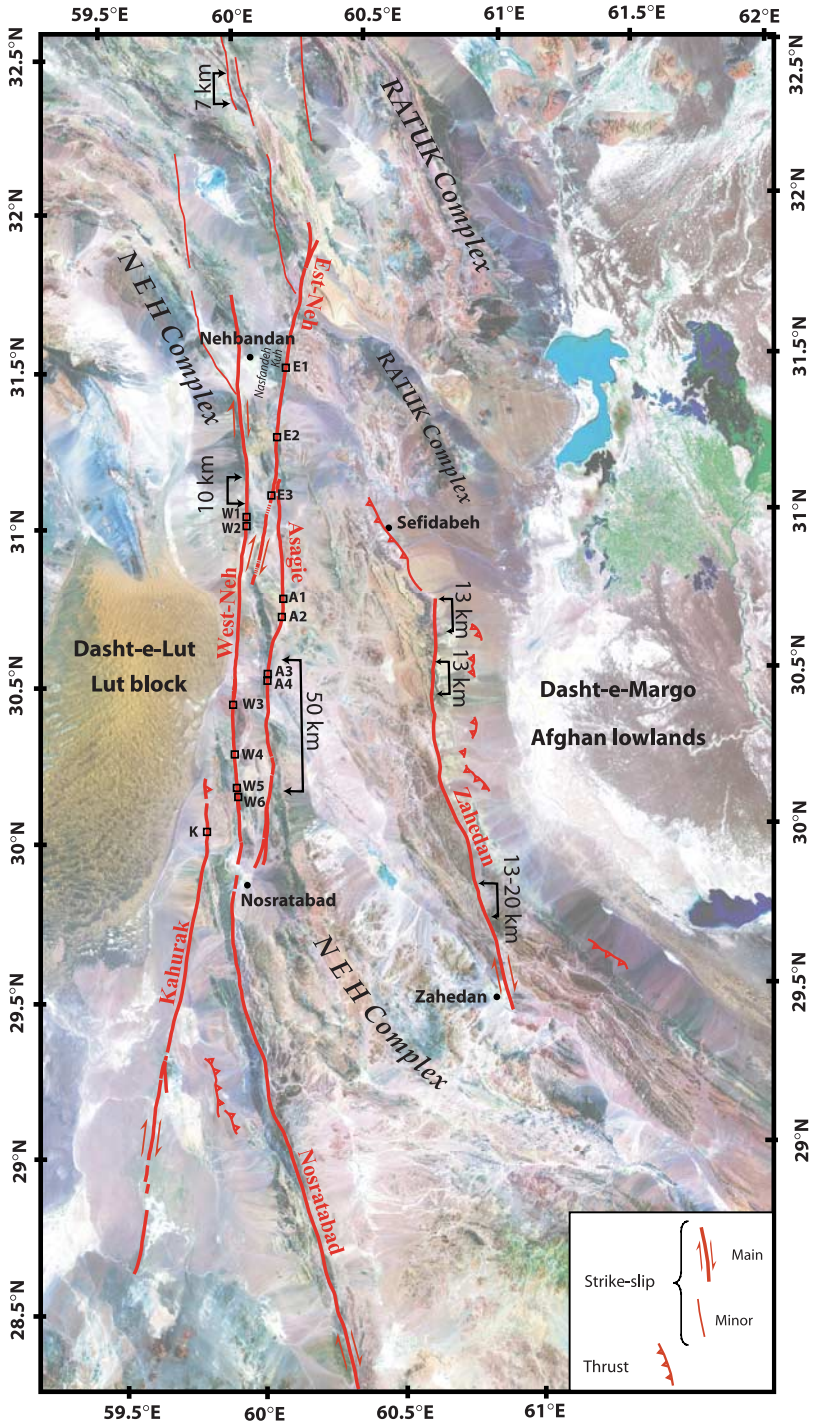

Figure 7. LANDSAT Mosaic of the Sistan region. Several parallel right-lateral faults displace units of the Sistan suture (Neh and Ratuk accretionary prism complexes). Geologic offsets are reported from *Walker and Jackson* [2004]. Boxes refer to sites with recent Quaternary offsets described in Figures 8–11.

portions of the northern one. Site A3 locates about 20 km to the south of A2. The trace of the fault that runs in the middle of Figure 9c separates basement to the west from a Quaternary piedmont to the east. The enlargement points to an abandoned alluvial fan whose surface (dark brown areas) has been incised by several narrow gullies and by one larger stream whose floodplain is denoted by light-blue hues. Both the gullies and the stream are deflected in a right lateral sense when crossing the fault trace, and restoring ~25 m of fault-motion aligns the upstream and downstream portions of the

Table 2. Geographic Coordinates of Offsets Used to Estimate Holocene Slip-Rates for the Deshir, Anar, and East Lut Fault Systems[a]

	Site	Latitude, °N	Longitude, °E	Offset, m	Type of Marker
Anar fault	site 1	31°16′11″	55°7′59″	7.5	river bank
	site 2	31°11′59″	55°9′8″	7.5–8	river bank
		31°11′26″	55°9′18″	15–20	channels
Deshir fault	*Deshir 1*	*30°38′23″*	*54°1′20″*	*25*	*offset streams*
	Deshir 2	*30°26′54″*	*54°7′23″*	*25*	*river bank*
Est-Neh fault	E1	31°29′34″	60°10′6″	25	fan edge
	E2	31°16′21″	60°7′39″	25	river incision
	E3	31°5′40″	60°6′18″	25	offset stream
Asagie fault	A1	30°45′50″	60°8′3″	25	streams and ridges
	A2	30°42′21″	60°7′51″	25	offset stream
	A2	30°42′15″	60°7′48″	25	offset stream
	A3	30°31′14″	60°4′15″	25	river incision
	A4	30°30′27″	60°4′11″	15	river incision
West-Neh fault	W1	31°1′11″	60°0′28″	20	fan edge
	W2	31°0′1″	60°0′22″	25	fan edge
	W3	30°26′12″	59°56′28″	45	fan edge and stream offset
	W4	30°16′23″	59°56′29″	50	canyon offset
	W5	30°9′50″	59°56′51″	25	offset streams
	W6	30°8′23″	59°56′59″	15	offset streams
Kahurak fault	K	30°2′4″	59°50′8″	35	offset stream

[a]The amount of offset and the nature of the marker are indicated in the two last columns. Sites along a given fault are ordered from the north (see graphical locations on Figures 5 and 7). Values for the Deshir fault are reported from *Meyer et al.* [2006] and italicized.

river-floodplain. Site A4 locates 2 km south of A3. The fault runs N-S in the middle of the SPOT5 extract (Figure 9d). To the north and to the south of the extract, the fault separates basement to the west from a Quaternary piedmont to the east. By the center of the extract, the fault cuts across the upper reach of the fans that mantle the piedmont. The enlargement shows the incision of the recent fan system (light grey and blue hues) within remnants of older systems (dark brown hue). The dextral deflection of the incision indicates a ~15 m offset, smaller than at sites A1–3.

[12] The West Neh fault neighbors and parallels the East Neh and Asagie fault along much of their lengths (Figure 7). Six sites distributed along the fault display a wider range of recent offsets than for the East Neh and Asagie faults. The offsets that postdate the last incision of the network vary between 15 m and 50 m (W1–W6 in Figure 6, and Table 2). Offsets of 20-25 m are found along the northern and central portions of the fault (sites W1 and W2). Greater offsets are found along the southern portion of the fault (sites W3 and W4), northeast of the northern tip of the Kahurak fault. At Site W1, the West Neh fault separates basement rocks to the East from a west dipping piedmont to the west (Figure 10a). By the center of the extract, the fault cuts and displaces the upper reach of a recent fan system. The enlargement shows a right-lateral offset of the northern edge of the fan that can be removed when restoring about 20 m of dextral fault-motion. Site W2 locates 3 km further to the south where the West Neh fault cuts across a Quaternary pediment (Figure 10b). The enlargement shows an old alluvial surface (dark blue) incised by small streams merging with the main river floodplains (light grey). The circle denotes remains of the old surfaces with a possible offset of 25 m that has accumulated since its incision by small streams. Site W3 locates 60 km further to the south where the Quaternary piedmont is cut and displaced by the fault (Figure 10c). Several alluvial fans that have been emplaced by streams flowing to the west can be distinguished. The remains of an old alluvial fan appear with dark brown hues in the center of the extract. The old fan is incised by the active alluvial surfaces and the river floodplains denoted with light grey colors. The southern edge of the old fan is cleanly offset because it has been preserved from erosion while active streams have smoothed the offset of the northern edge close to the fault. Restoring about 45 m of dextral fault-motion removes the bayonet-shaped portions of the southern incision and aligns the upstream and downstream floodplains of the recent fan system. Site W4 locates about 20 km further to the south and provides a similar offset. There, the fault cuts across old alluvial surfaces mantling basement rocks (Figure 10d). The oldest surface (dark blue) is made of material collected from ultrabasites cropping out further to the east. An intermediate surface (light brown) is made of material collected from Eocene rocks. Both surfaces are inactive and have been incised by the rivers whose floodplains appear as narrow stripes with light blue or grey hues. The river in the center of the extract flows to the west into a narrow canyon. The sharp offset of the canyon close to the fault postdates the emplacement of the alluvial surfaces and the incision of bedrock. The offset amounts to ~50 m and has accumulated since the last network incision. Sites W5 and W6 locate 15 km to the south by the portion of the West Neh fault that overlaps with the Kahurak fault and they provide smaller values of recent offsets. At site W5, the fault cuts across an east-dipping pediment mantling basement rocks (Figure 10e). The active fan system, denoted by light brown hues, covers most of the pediment to the south. An older system is outlined by dark brown areas and covers most of the piedmont to the north. Many small streams have

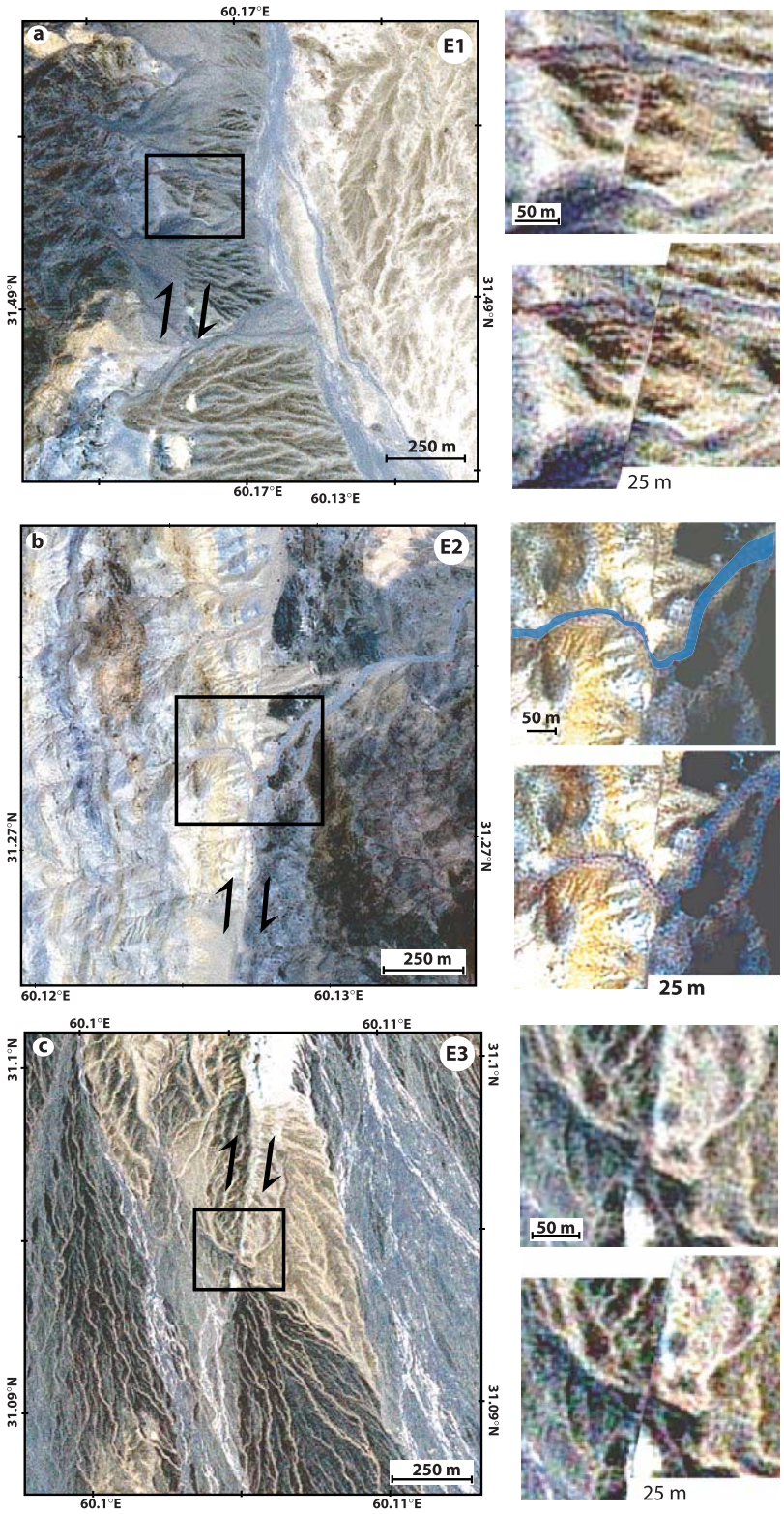

Figure 8. Late Quaternary offsets postdating the recent incision of the network along the East Neh fault. Sites are located on Figure 7. Boxes denote enlarged areas (top panels) with right-lateral motion restored (bottom panels).

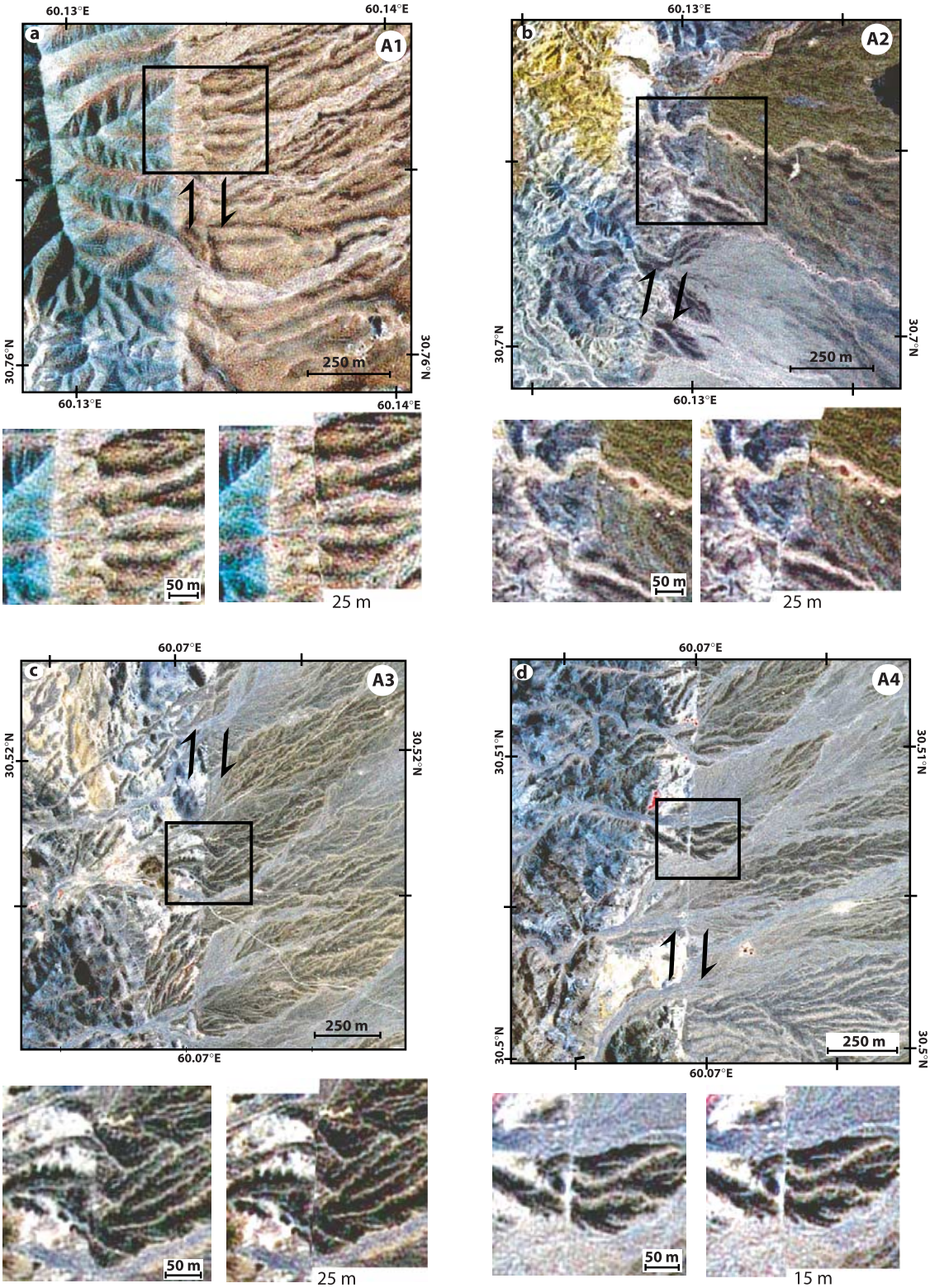

Figure 9. Late Quaternary offsets postdating the recent incision of the network along the Asagie fault. Sites are located on Figure 7. Boxes denote enlarged areas (left panels) with right-lateral motion restored (right panels).

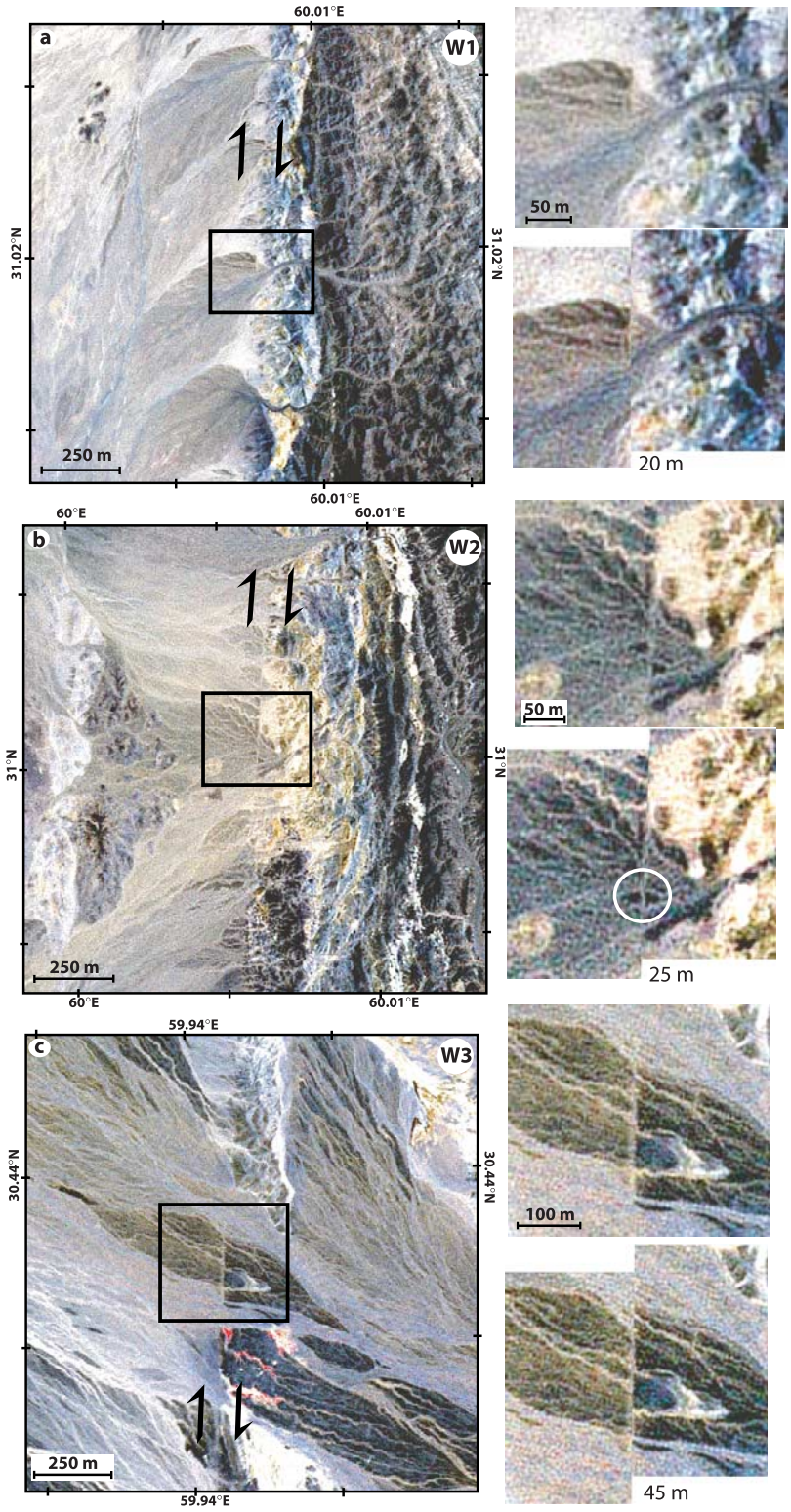

Figure 10. Late Quaternary offsets postdating the recent incision of the network along the West Neh fault. Sites are located on Figure 7. Boxes denote enlarged areas (top panels) with right-lateral motion restored (bottom panels).

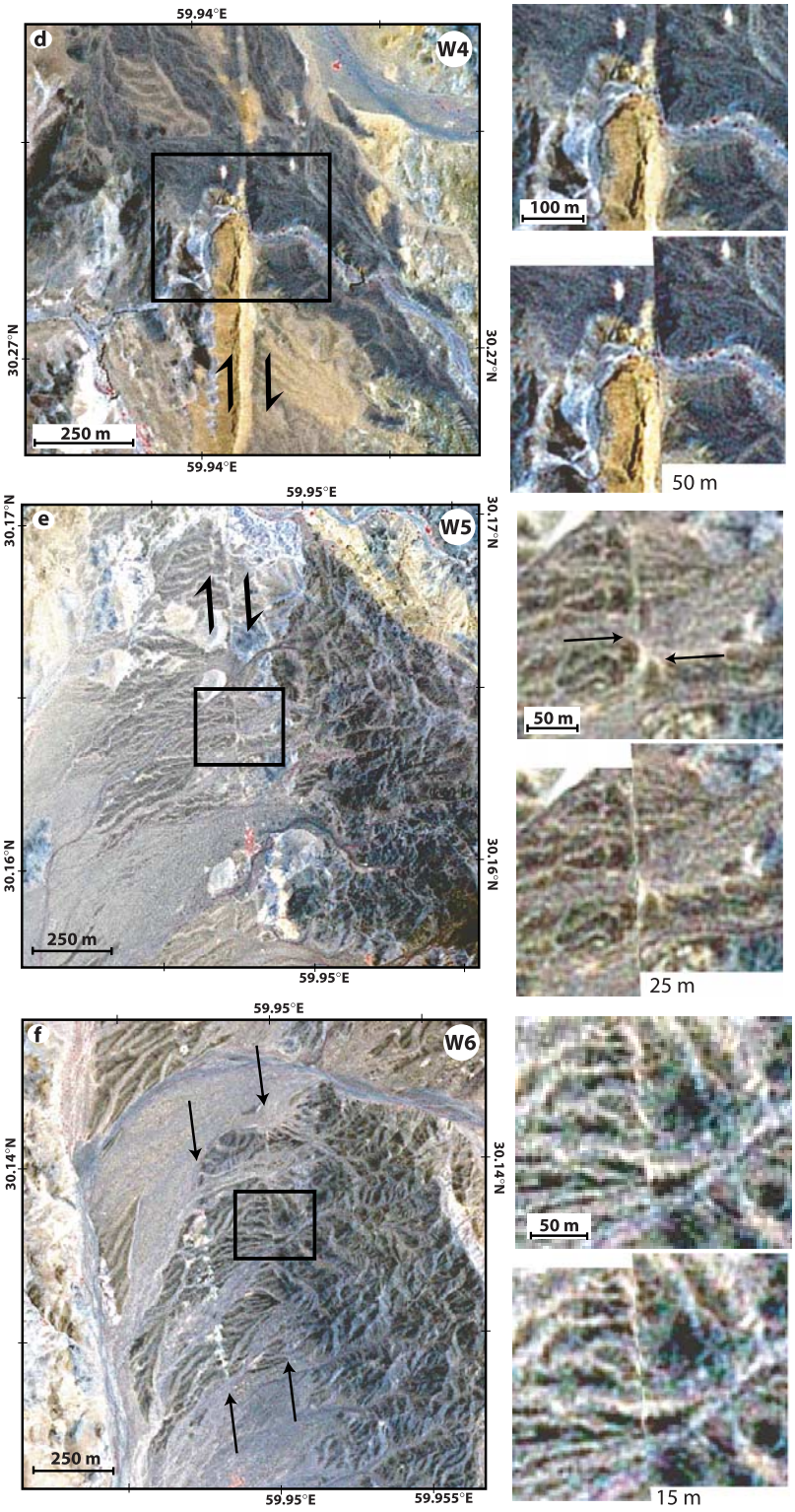

Figure 10. (continued)

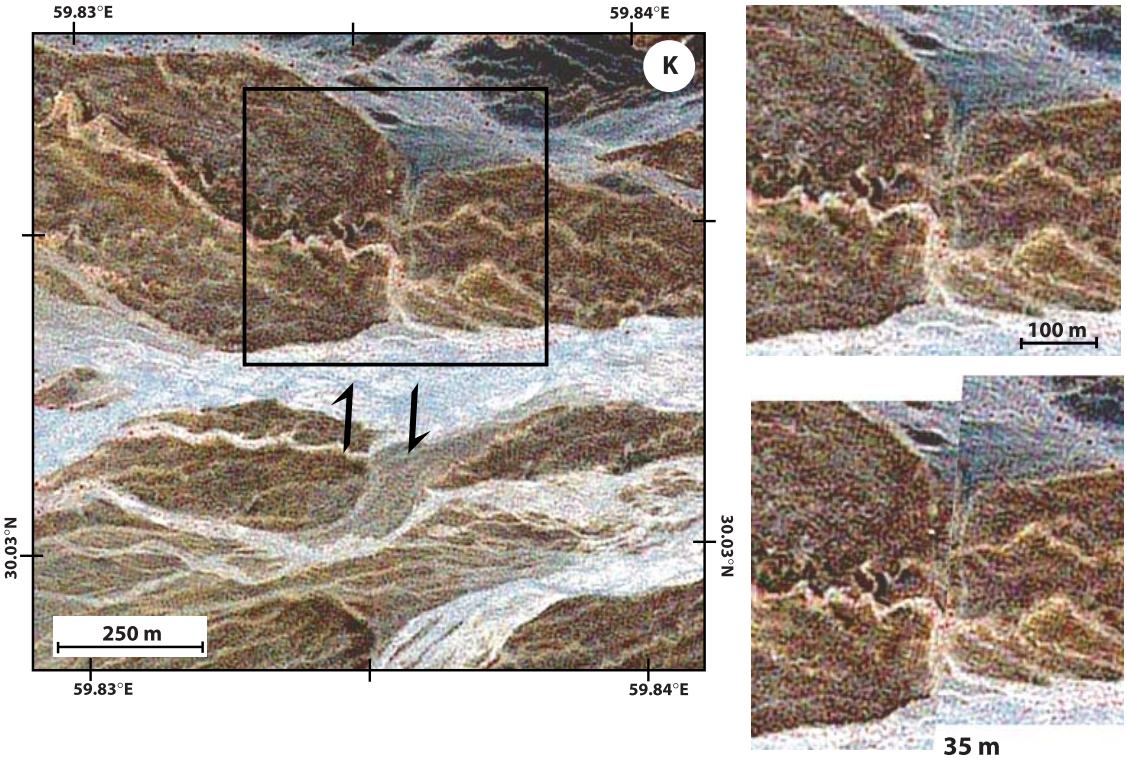

Figure 11. Late Quaternary offset postdating the recent incision of the network along the Kahurak fault. The site is located on Figure 7. Boxes denote enlarged areas (top panels) with right-lateral motion restored (bottom panels).

dissected the older fans to merge with the floodplains of the active network and several ones display a clear right-lateral offset. The enlargement points to one of these offsets with the arrows indicating the riser between the abandoned and active fans. Restoring about 25 m of fault-motion aligns the upstream and downstream portions of the risers and removes the morphologic offset. At site W6, the West Neh fault cuts across a west-dipping Quaternary piedmont. The fault is made of two parallel splays (arrows on Figure 10f) that merge into a single strand to the north and to the south of the extract. The splays cut across an active fan system (light grey) that has dissected an older fan (dark blue). Remnants of the older fan have been preserved close to the center of the SPOT5 extract. The enlargement shows ~15 m of dextral-offset along the eastern splay. The offset postdates the incision by the many small streams merging downstream with the active alluvial surfaces. This value does not account for a possible contribution of the western splay, and provides a minimum estimate for the slip accumulated since the incision.

[13] The Kahurak fault locates to the southwest of the West Neh fault. The northern portion of the Kahurak fault and the southern portion of the West Neh fault overlap over a 30 km long distance (Figure 7). Clues for recent motion are found at one site by the southern end of the overlapping region. Site K locates by 30°N where the Kahurak fault cuts across a series of alluvial fans (Figure 11). Several abandoned alluvial surfaces have brown and beige hues that distinguish from the main river floodplains denoted by blue or white colors. The detail shows a meandering stream within the surface of an old fan with a course compatible with an offset of 35 m. Restoring that amount of dextral motion realigns the northern edge of the fan surface but deconstructs its southern edge. This may result from a rejuvenated incision by the active riser along the main river floodplain, east of the fault.

5. Climate Evolution and Likely Age of the Recent Offsets

[14] The former observations indicate active strike-slip faulting occurs along the eastern edge of the Lut as well as within the Iranian plateau, along the Anar fault. Most of the offsets documented record the slip accumulated across imbricate fans since the last incision of the network. Neither the fans nor the offset-levels have been accurately dated precluding simple slip-rate calculations. Estimates of the slip-rates can be nonetheless inferred from the evolution of similar well-dated fan systems in three other places of Iran. The more complete description concerns faulted piedmonts along the Sabzevaran and Minab fault zones, in SE Iran, where four generations of Pleistocene alluvial fans have been correlated over vast areas [*Regard et al.*, 2004, 2005]. The youngest generation of the fans has been dated with ^{10}Be cosmogenic method and the abandonment of alluvial surfaces appears to correlate with global climate changes [*Regard et al.*, 2006]. *Regard et al.* [2006] document five

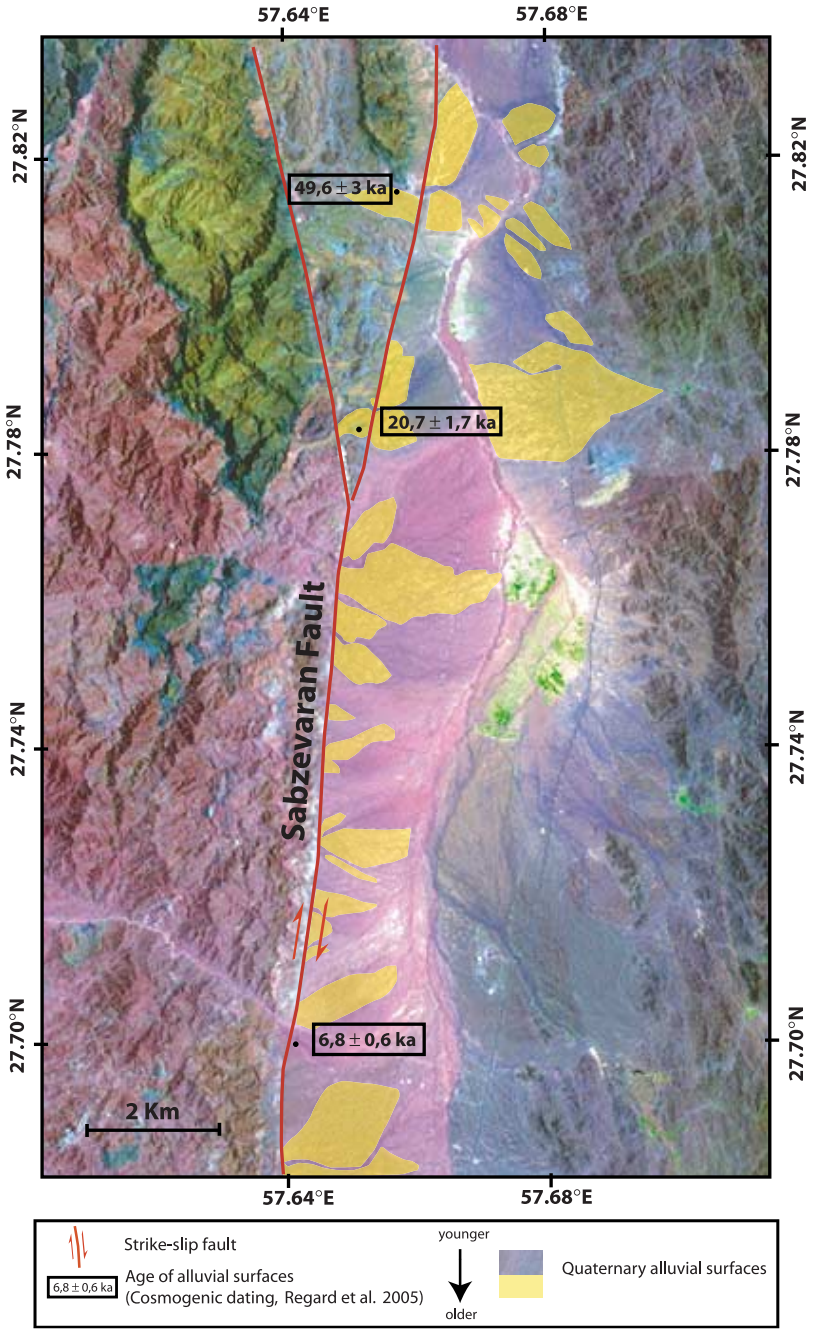

Figure 12. LANDSAT enlargement of the Sabzevaran fault with cosmogenic exposure ages reported from *Regard et al.* [2006]. Distinctive alluvial surfaces typify the faulted piedmont. Main river floodplains and intermittent braided channels incise the inactive parts (yellow shading) of the recent fan system. Available dating suggests a Late Pleistocene aggradation of the fans and a later regional incision.

inset levels with surface ages clustering around ~6, ~8, ~13, ~20, and ~45 ka. The ages obtained for the Sabzevaran fault are reported on a LANDSAT image distinguishing current depositional lobes from inactive parts of the recent fan system (Figure 12). The ages gathered on the inactive parts of the fans are all older than the Late Glacial Maximum while ages obtained on the still active parts of the fans are all younger. The age distribution suggests that the fans were emplaced during the last glacial period (Würm) with successive phases of aggradation lasting until the end of the Late Glacial Maximum, about 20 ka ago. The fans have been subsequently incised by the onset of Holocene global warming, about 12 ± 2 ka ago, with large remains of the Würm surfaces preserved upstream. Several levels dated at ~6–8 ka [*Regard et al.*, 2006] relate to the Holocene climatic optimum and are imbricated within the Early Holocene incision. The Holocene levels emplaced mostly downstream by fan-head entrenchment and outline the

active drainage system. The drastic change between the Würm aggradation and the Holocene incision has also been documented in north Iran. *Fattahi et al.* [2006a] have studied a portion of the Sabzevar thrust (SB on the inset Figure 2) warping a gently south-dipping piedmont. The fault disrupts a thick sequence of fanglomerates whose surface is perched ~10 m above the base level of the active streambed and intermittent tributaries. Optically Stimulated Luminescence (OSL) dating indicates that the youngest fanglomerates emplaced between 30 to 13 ka before the onset of an ongoing period of erosion [*Fattahi et al.*, 2006a]. A similar situation has been described for the Doruneh strike-slip fault where Infrared Stimulated Luminescence (IRSL) dating of inset terraces indicates a shift from depositional to erosional conditions by ~10 ka [*Fattahi et al.*, 2006b]. The last significant incision therefore appears coeval with the onset of the Holocene in northern and southern Iran, and we think there is little, if any, reason for a different situation in central and eastern Iran.

[15] The recent evolution of climate in Iran also resembles that documented in other places of the deforming Eurasia where the Holocene warming has affected the geomorphology. It has long been proposed that a sudden change of the erosional conditions, thought to be coeval with the onset of the last deglaciation and the beginning of the Holocene, triggered widespread incision and shaped characteristic morphologies from the Mediterranean lowlands [e.g., *Armijo et al.*, 1992] up to the Tibetan plateau [e.g., *Armijo et al.*, 1986]. Further studies provided accurate dating and substantiated the morphologic imprint of the early Holocene incision in and around Tibet [e.g., *Van der Woerd et al.*, 1998, 2002; *Hetzel et al.*, 2004, 2006; *Mériaux et al.*, 2005], in the Aegean [*Benedetti et al.*, 2002, 2003] and across Italy [*Palumbo et al.*, 2004]. The former discussions make it reasonable to state that the onset of the Holocene global warming, associated with a drastic change in the sedimentation of the Persian Gulf [*Uchupi et al.*, 1999], has affected the landscape of Iran.

[16] The striking similarities between the morphologies of the imbricate fans that mantle the Anar, Deshir, West Neh and Sabzevaran piedmonts, together with the dates available for the Sabzevaran alluvial fans, suggest an early Holocene age of the latest regional incision. The offsets of the morphologic features we have described are inherited from that latest incision. Theses offsets have probably recorded fault motion since the beginning of the Holocene and can be used to estimate slip-rates over the last 12 ± 2 ka. Based on the offsets reported in this study, the slip-rates would be ~0.5–0.75 mm/yr, ~1.75–2.5 mm/yr, ~1–5 mm/yr, ~1–2.5 mm/yr for the Anar, East Neh, West Neh, and Asagie faults, respectively (Table 2 and Figure 3). Similarly, the site found along the Kahurak fault would indicate a rate of ~2.5–3.5 mm/yr for its northern portion but the single offset on which it is based makes this estimate unreliable.

6. Discussion and Conclusion

[17] The rates we have estimated for the Anar, East Neh, West Neh, and Asagie faults rely on a coherent morphoclimatic scenario, but they need to be checked by direct dating of the offset-fan surfaces. Without such direct dating, one cannot rule out possibilities for greater slip-rates if the incisions relate to the Holocene optimum (~6–8 ka) and for smaller slip-rates if the incisions predate the Holocene global warming. Because there is only one episode of regional incision for many of the sites we have described, we have assumed it relates rather to the largest and most recent climate change, the onset of the Holocene, than to less prominent climatic events. While the fault slip-rates estimated over the Holocene remain speculative, they offer a comparison with the very long-term estimates by *Walker and Jackson* [2004]. The Holocene dextral shear accumulated across the East Neh and West Neh faults would be about ~2.75–7.5 mm/yr near 30.5°N. To match the ~14 mm/yr anticipated by *Walker and Jackson* [2004] across the Eastern Lut fault system, the Holocene slip-rate across the Zahedan fault would have to be of 6.5 mm/yr at least. Although we lack high-resolution SPOT5 images along the Zahedan fault, it is unlikely that this fault, with length similar to and total offset smaller than the Anar fault, slips at such a rate. If the 16 mm/yr of differential GPS motion evidenced across the Lut do extrapolate to geologic timescales, hidden faults inside the Lut must have to account for a large part of the remaining shear. If not, GPS data have incorporated transient effects possibly associated with a strong coupling at the Makran subduction interface. The former alternative seems unlikely since the Lut is devoid of seismicity and behaves as a rather rigid block. The latter alternative suggests in turn that the 5 Ma-old age assumed for the inception of strike-slip faulting might be too young and needs revision. Assuming our Holocene estimates are correct and remained constant since the onset of motion, the total offset of 60 km across the Neh faults would have accrued over the last 8–22 Ma at overall rates of ~2.75–7.5 mm/yr. This is not in contradiction with recent studies constraining the onset of strike-slip faulting in the Kopeh Dagh [*Hollingsworth et al.*, 2006] and that of rapid exhumation in the Alborz mountains [*Guest et al.*, 2006] at 10 and 12 Ma, respectively.

[18] While the Holocene slip-rate summed across the Sistan faults is smaller than the long-term estimates of *Walker and Jackson* [2004], it is close to the GPS-derived estimate proposed by *Reilinger et al.* [2006]. The latter have modeled the GPS data with a rigid block formalism allowing for intersismic strain accumulation along the block boundaries. They derive a right-lateral slip of 5.5 mm/yr along the N-S boundary of the Sistan suture zone [see *Reilinger et al.*, 2006, Figure 9c]. This result however is influenced by the position and the amount of slip of adjacent block-boundaries, specifically the NE-SW boundary connected to the West Lut and located immediately north of the vector KERM (Figure 3). The latter boundary that cuts obliquely across the Anar fault requires a shortening of ~6 mm/yr, as much as across the entire Zagros, and a dextral slip of ~5.5 mm/yr, almost twice the rate of the Nayband fault. While some distributed shortening is indeed documented in the Kerman province [*Walker*, 2006] with interacting thrust and strike-slip faults able to produce *Mw*

$\sim$ 6.5 earthquakes [e.g., *Talebian et al.*, 2006], this limited deformation cannot account for the amounts of shortening and strike-slip required on the former boundary. While the East and West Lut boundaries are geologically reasonable, have a long-term history of motion and show clear morphological evidence of recent activity, this is not the case for the boundary cutting across the Anar fault. This casts some doubts on the slip-rates whose estimates are tied to this boundary. Our understanding of the recent tectonics of Iran will long remain subordinate to a better knowledge of geodetic and geologic slip-rates. This requires longer GPS observations and denser networks designed to retrieve the intersismic strain across individual faults, as recently done for the Minab fault zone [*Bayer et al.*, 2006], as well as extensive sampling and accurate dating of well-constrained offset-morphologies. The sites described in the present-study offer a number of morphological offsets that should be targeted for a better assessment of the seismic hazard in Eastern Iran.

[19] **Acknowledgments.** CNES and SPOT Image (ISIS program contracts ISIS0403-622 and ISIS0510-812) made available the SPOT5 data used in this study. PNTS provided additional funding for the Quickbird imagery. Figure 2 has been produced using the GMT software [*Wessel and Schmidt*, 1995]. We are grateful to Mohammad Foroutan for efficient organisation of our short field trip to the Anar fault and indebted to the Geological Survey of Iran for supporting our work. We acknowledge helpful and detailed reviews by Manuel Berberian, Vincent Regard, and an anonymous reviewer. The sharp but constructive criticisms by the anonymous reviewer helped to improve the presentation and the discussion of the data, but we alone are responsible for remaining inaccuracies and errors.

References

Agard, P., J. Omrani, L. Jolivet, and F. Mouthereau (2005), Convergence history across Zagros (Iran): Constraints from collisional and earlier deformation, *Int. J. Earth Sci.*, *94*, 401–419.

Agard, P., P. Monié, W. Gerber, J. Omrani, M. Molinaro, B. Meyer, L. Labrousse, B. Vrielynck, L. Jolivet, and P. Yamato (2006), Transient syn-obduction exhumation of Zagros blueschists inferred from P-T-deformation-time-kinematics constraints: Implications for the Neotethyan wedge dynamics, *J. Geophys. Res.*, *111*, B11401, doi:10.1029/2005JB004103.

Allen, M., J. Jackson, and R. Walker (2004), Late Cenozoic reorganization of the Arabia-Eurasia collision and the comparison of short-term and long-term deformation rates, *Tectonics*, *23*, TC2008, doi:10.1029/3003TC001530.

Armijo, R., P. Tapponnier, J. L. Mercier, and H. Tonglin (1986), Quaternary extension in southern Tibet: Field observations and tectonic implications, *J. Geophys. Res.*, *91*, 13,803–13,872.

Armijo, R., P. Tapponnier, and H. Tonglin (1989), Late Cenozoic right-lateral strike-slip faulting in southern Tibet, *J. Geophys. Res.*, *94*, 2787–2838.

Armijo, R., H. Lyon-Caen, and D. Papanastassiou (1992), East-west extension and Holocene normal-faults scarps in the Hellenic arc, *Geology*, *20*, 491–494.

Avouac, J. P., and P. Tapponnier (1993), Kinematic model of active deformation in central Asia, *Geophys. Res. Lett.*, *20*(10), 895–898.

Bayer, R., J. Cry, M. Tatar, P. Vernant, M. Abbassi, F. Masson, F. Nilforoushan, E. Doerflinger, V. Regard, and O. Bellier (2006), Active deformation in Zagros-Makran transition zone inferred from GPS measurements, *Geophys. J. Int.*, *165*, 373–381.

Bendick, R., R. Bilham, J. Freymueller, K. Larson, and G. H. Yin (2000), Geodetic evidence for a low slip-rate in the Altyn Tagh fault system, *Nature*, *404*(6773), 69–72.

Benedetti, L., R. Finkel, D. Papanastassiou, G. King, R. Armijo, F. Ryerson, D. Farber, and F. Flerit (2002), Post-glacial slip history of the Sparta fault (Greec) determined by 36Cl cosmogenic dating: Evidence for non-periodic earthquakes, *Geophys. Res. Lett.*, *29*(8), 1246, doi:10.1029/2001GL014510.

Benedetti, L., R. Finkel, G. King, R. Armijo, D. Papanastassiou, F. Ryerson, F. Flerit, D. Farber, and G. Stavrakakis (2003), Motion on the Kaparelli fault (Greece) prior to the 1981 earthquake sequence determined from 36Cl cosmogenic dating, *Terra Nova*, *15*(2), 118–124.

Berberian, F., and M. Berberian (1981), Tectono-Plutonic episodes in Iran, in *Zagros, Hindu Kush, Himalaya: Geodynamic evolution*, *Geodyn. Ser.*, vol 3, edited by H. K. Gupta and F. M. Delany, pp. 5–33.

Berberian, M., and G. C. P. King (1981), Towards a paleogeography and tectonic evolution of Iran, *Can. J. Earth Sci.*, *18*, 210–265.

Berberian, F., I. D. Muir, R. J. Pankhurst, and M. Berberian (1982), Late Cretaceous and Early Miocene Andean-type plutonic activity in northern Makran and Central Iran, *J. Geol. Soc.*, *139*, 605–614.

Berberian, M., J. A. Jackson, M. Qorashi, M. M. Khatib, K. Priestley, M. Talebian, and M. Ghafuri-Ashtiani (1999), The 1997 May 10 Zirkuh (Qa'enat) earthquake (Mw 7.2): Faulting along the Sistan suture zone of eastern Iran, *Geophys. J. Int.*, *136*, 671–694.

Berberian, M., J. A. Jackson, M. Qorashi, M. Talebian, M. M. Khatabi, and K. Priestley (2000), The 1994 Sefidabeh earthquakes in eastern Iran: Blind thrusting and bedding-plane slip on a growing anticline, and active tectonics of the Sistan Suture zone, *Geophys. J. Int.*, *142*, 283–299.

Burov, E. B., and A. B. Watts (2006), The long-term strength of continental lithosphere: "Jelly sandwich" or "crème brûlée"?, *GSA Today*, *16*, 4–10.

England, P., and D. McKenzie (1982), A thin viscous sheet model for continental deformation, *Geophys. J. R. Astro. Soc.*, *70*, 295–321.

England, P., and P. Molnar (1997), The field of crustal velocity in Asia calculated from Quaternary rates of slip on faults, *Geophys. J. Int.*, *130*(3), 551–582.

Fattahi, M., R. Walker, J. hollingsworth, A. Bahroudi, H. Nazari, M. Talebian, S. Armitage, and S. Stokes (2006a), Holocene slip-rate on the Sabzevar thrust fault, NE Iran, determined using optically stimulated luminescence (OSL), *Earth Planet. Sci. Lett.*, *245*, 673–684.

Fattahi, M., R. Walker, M. Khatib, A. Dolati, and A. Bahroudi (2006b), Slip-rate estimate and past earthquakes on the Doruneh fault, eastern Iran the Sabzevar thrust fault, NE Iran, *Geophys. J. Int.*, *168*(2), 691–709.

Friedrich, A. M., B. Wernicke, N. A. Niemi, R. A. Bennett, and J. L. Davis (2003), Comparison of geodetic and geologic data from the Wasatch region, Utah, and implications for the spectral character of Earth deformation at periods of 10 to 10 million years, *J. Geophys. Res.*, *108*(B4), 2199, doi:10.1029/2001JB000682.

Guest, B., D. E. Stockli, M. Grove, G. J. Axen, P. S. Lam, and J. Hassanzadeh (2006), Thermal histories from the central Alborz Mountains, northern Iran: Implications for the spatial and temporal distribution of deformation in northern Iran, *Geol. Soc. Am. Bull.*, *118*, 1507–1521.

Hetzel, R., M. Tao, S. Stokes, S. Niedermann, S. Ivy-Ochs, B. Gao, M. R. Strecker, and P. W. Kubik (2004), Late Pleistocene/Holocene slip-rate of the Zhangye thrust (Qilian Shan, China) and implications for the active growth of the northeastern Tibetan Plateau, *Tectonics*, *23*, TC6006, doi:10.1029/2004TC001653.

Hetzel, R., S. Niedermann, M. Tao, P. W. Kubik, and M. R. Strecker (2006), Climatic versus tectonic control on river incision at the margin of NE Tibet: 10Be exposure dating of river terraces at the mountain front of the Qilian Shan, *J. Geophys. Res.*, *111*, F03012, doi:10.1029/2005JF000352.

Hollingsworth, J., J. Jackson, R. Walker, M. R. Gheitanchi, and M. J. Bolourchi (2006), Strike-slip faulting, rotations, and along strike elongation in the Kopeh Dagh mountains, NE Iran, *Geophys. J. Int.*, *166*, 1161–1177.

Homke, S., J. Vergés, M. Garcés, H. Emami adn, and R. Karpuz (2004), Magnetostratigraphy of Miocene-Pliocene Zagros foreland deposits in the front of Push-e Kush Arc (Lurestan Province, Iran), *Earth Planet. Sci. Lett.*, *225*, 397–410.

Jackson, J. (2002), Strength of the continental lithosphere: Time to abandon the jelly sandwich?, *GSA Today*, *12*(9), 4–10.

Leloup, P. H., R. Lacassin, P. Tapponnier, D. Zhong, X. Liu, L. Zhang, S. Ji, and P. T. Trinh (1995), The Ailao Shan-Red River shear zone (Yunnan, China), Tertiary transform boundary of Indochina, *Tectonophysics*, *251*, 3–84.

Mériaux, A.-S., F. J. Ryerson, P. Tapponnier, J. Van der Woerd, R. C. Finkel, X. Xu, Z. Xu, and M. W. Caffee (2004), Rapid slip along the central Altyn Tagh Fault: Morphochronologic evidence from Cherchen He and Sulamu Tagh, *J. Geophys. Res.*, *109*, B06401, doi:10.1029/2003JB002558.

Mériaux, A.-S., P. Tapponnier, F. J. Ryerson, X. Xu, G. King, J. Van der Woerd, R. C. Finkel, H. Li, M. W. Caffee, Z. Xu, and C. Wenbin (2005), The Aksay segment of the Northern Altyn Tagh fault: Tectonic Geomorphology, Landscape Evolution and Holocene slip-rate, *J. Geophys. Res.*, *110*, B04404, doi:10.1029/2004JB003210.

Meyer, B., P. Tapponnier, L. Bourjot, F. Métivier, Y. Gaudemer, G. Peltzer, G. Shunmin, and C. Zhitai (1998), Crustal thickening in Gansu-Qinghai, lithospheric mantle subduction, and oblique, strike-slip controlled growth of the Tibet Plateau, *Geophys. J. Int.*, *135*, 1–47.

Meyer, B., F. Mouthereau, O. Lacombe, and P. Agard (2006), Evidence of Quaternary activity along the Deshir fault: Implication for the Tertiary tectonics of Central Iran, *Geophys. J. Int.*, *164*, 192–201.

Molnar, P., and P. Tapponnier (1975), Cenozoic tectonics of Asia: Effects of a continental collision, *Science*, *4201*, 419–426.

Nabavi, M. H. (1970), Geological Map of Yazd sheet (H9), scale 1:250,000, Geol. Surv. of Iran, Teheran.

Palumbo, L., L. Benedetti, D. Bourlès, A. Cinque, and R. Finkel (2004), Slip history of the Magnola Fault

(Apennines, Central Italy) from 36Cl surface exposure dating: Evidence for strong earthquakes over the Holocene, *Earth Planet. Sci. Lett.*, *225*, 163–176.

Peltzer, G., P. Tapponnier, and R. Armijo (1989), Magnitude of Late Quaternary left-lateral displacements along the north edge of Tibet, *Science*, *246*, 1285–1289.

Regard, V., O. Bellier, J.-C. Thomas, M. R. Abbassi, J. Mercier, E. Shabanian, K. Feghhi, and S. Soleymani (2004), Accommodation of Arabia-Eurasia convergence in the Zagros-Makran transfer zone, SE Iran: A transition between collision and subduction through a young deforming system, *Tectonics*, *23*, TC4007, doi:10.1029/2003TC001599.

Regard, V., O. Bellier, J.-C. Thomas, D. Bourlès, S. Bonnet, M. R. Abbassi, R. Braucher, J. Mercier, E. Shabanian, Sh. Soleymani, and Kh. Feghhi (2005), Cumulative right-lateral fault slip-rate across the Zagros - Makran transfer zone: Role of the Minab-Zendan fault system in accommodating Arabia-Eurasia convergence in SE Iran, *Geophys. J. Int.*, *162*, 177–203.

Regard, V., O. Bellier, R. Braucher, F. Gasse, D. Bourlès, J. Mercier, J.-C. Thomas, M. R. Abbassi, E. Shabanian, and Sh. Soleymani (2006), 10Be dating of alluvial deposits from Southeastern Iran (the Hormoz Strait area), *Palaeogeogr. Palaeoclimatol. Palaeoecol.*, *242*, 36–53.

Reilinger, R., et al. (2006), GPS constraints on continental deformation in the Africa-Arabia-Eurasia continental collision zone and implications for the dynamics of plate interactions, *J. Geophys. Res.*, *111*, B05411, doi:10.1029/2005JB004051.

Sella, G. F., T. H. Dixon, and A. Mao (2002), REVEL: A model for recent plate velocities from space geodesy, *J. Geophys. Res.*, *107*(B4), 2081, doi:10.1029/2000JB000033.

Talebian, M., and J. Jackson (2002), Offset on the Main Recent Fault of NW Iran and implications for the late Cenozoic tectonics of the Arabia-Eurasia collision zone, *Geophys. J. Int.*, *150*, 422–439.

Talebian, M., and J. Jackson (2004), A reappraisal of earthquake focal mechanisms and active shortening in the Zagros mountains of Iran, *Geophys. J. Int.*, *156*, 506–526.

Talebian, M., J. Biggs, M. Bolourchi, A. Copley, A. Ghassemi, M. Ghorashi, J. Hollingsworth, J. Jackson, E. Nissen, B. Oveisi, B. Parsons, K. Priestley, and A. Saiidi (2006), The Dahuiyeh (Zarand) earthquake of 2005 February 22 in central Iran: Reactivation of an intramountain reverse fault, *Geophys. J. Int.*, *164*(1), 137–148, doi:10.1111/j.1365-246X.2005.02839.x.

Tapponnier, P., and P. Molnar (1977), Active faulting and tectonics in China, *J. Geophys. Res.*, *82*(20), 2905–2930.

Tapponnier, P., G. Peltzer, A. Y. Le Dain, R. Armijo, and P. Cobbold (1982), Propagating extrusion tectonics in Asia: New insights from simple experiments with plasticine, *Geology*, *10*, 611–616.

Tirrul, R., I. R. Bell, R. J. Griffis, and V. E. Camp (1983), The Sistan suture zone of Eastern Iran, *Geol. Soc Am. Bull.*, *94*, 134–150.

Uchupi, E., S. A. Swift, and D. A. Ross (1999), Late Quaternary stratigraphy, paleoclimate and neotectonism of the Persian (Arabian) Gulf region, *Mar. Geol.*, *160*, 1–23.

Valeh, N., and A. Haghipour (1970), Geological Map of Ardekan, scale 1:250,000, Geological Survey of Iran, Tehran.

Van der Woerd, J. W., F. J. Ryerson, P. Tapponnier, Y. Gaudemer, R. Finkel, A. S. Meriaux, M. Caffee, G. G. Zhao, and Q. L. He (1998), Holocene left-slip rate determined by cosmogenic surface dating on the Xidatan segment of the Kunlun fault (Qinghai, China), *Geology*, *26*(8), 695–698.

Van der Woerd, J., P. Tapponnier, F. J. Ryerson, A. S. Mériaux, B. Meyer, Y. Gaudemer, R. Finkel, M. Caffee, G. Zhao, and Z. Xu (2002), Uniform post-glacial slip-rate along the central 600 km of the Kunlun Fault (Tibet), from 26Al, 10Be and 14C dating of riser offsets, and climatic origin of the regional morphology, *Geophys. J. Int.*, *148*, 356–388.

Vernant, Ph., F. Nilforoushan, D. Hatzfeld, M. R. Abassi, C. Vigny, F. Masson, H. Nankali, J. Martinod, A. Ashtiani, R. Bayer, F. Tavakoli, and J. Chery (2004), Present-day crustal deformation and plate kinematics in the Middle East constrained by GPS measurements in Iran and Northern Oman, *Geophys. J. Int.*, *157*, 381–398.

Walker, R. T. (2006), A remote sensing study of active folding and faulting in southern Kerman province, S. E. Iran, *J. Structural Geology*, *28*, 654–668.

Walker, R., and J. Jackson (2002), Offset and evolution of the Gowk fault, S.E. Iran: a major intra-continental strike-slip system, *J. Struc. Geol.*, *24*, 1677–1698.

Walker, R., and J. Jackson (2004), Tectonics of Central and Eastern Iran, *Tectonics*, *23*, TC5010, doi:10.1029/2003TC001529.

Wallace, K., G. Yin, and R. Bilham (2004), Inescapable slow slip on the Altyn Tagh fault, *Geophys. Res. Lett.*, *31*, L09613, doi:10.1029/2004GL019724.

Wessel, P., and W. H. F. Schmidt (1995), New version of the generic mapping tools released, *EOS Trans. Am. Geophys. Union*, *76*, 329.

Wright, T., B. Parsons, P. England, and E. Fielding (2004), InSAR observations of low slip-rates on the major faults of Western Tibet, *Science*, *305*, 236–239.

K. Le Dortz and B. Meyer, Laboratoire de Tectonique, Université Pierre et Marie Curie, Paris 6, CNRS, UCP, case 129–4 place Jussieu, 75252 Paris, France. (bmeyer@ccr.jussieu.fr)